Layer-by-layer synthesis of Zn-doped MnO$_2$ nanocrystals as cathode materials for aqueous zinc-ion battery

A. A. Lobinsky, M. V. Kaneva

Saint Petersburg State University, Peterhof, 198504 Saint Petersburg, Russia

lobinsky.a@gmail.com

This work first described the new oxidation-reduction route for the synthesis of Zn-doped MnO$_2$ nanocrystals via layer-by-layer method as cathode material for an aqueous zinc-ion battery. The obtained nanolayers were characterized by SEM, XRD, XPS and FTIR spectroscopy. The results show the synthesized nanolayers were formed from two-dimensional nanocrystals Zn$_{0.3}$MnO$_2$ the thickness of about 3–8 nm and the morphology of "nanosheets" with the birnessite-like crystal structure. Benefiting from the aqueous 2M ZnSO$_4$ electrolyte and Zn$_{0.3}$MnO$_2$ nanocrystals-based cathode, the zinc-ion battery delivers a high specific capacity (216 mAh/g at 1 A/g) and excellent cycling stability (95% capacity retention after 1000 charge-discharge cycles). The obtained results demonstrate the manganese oxide-based aqueous zinc-ion battery is a promising technology for powering next-generation electronics.

1. Introduction

In recent years, zinc-ion batteries are receiving much attention as low-cost and safe energy storage technology for emerging applications in flexible and safe devices [1]. However, deficiency of high energy-density electrode materials is now the main limit for obtaining high-performance zinc-ion batteries. Thus, the development of high-performance electrode materials is the key to improving the capacity and increase the commercial application of zinc-ion batteries [2–4].

The main function of a zinc-ion battery cathode is to provide a stable structure in which Zn^{2+} ions can be chemically bonded with low binding energy and fast kinetics [5]. Thus, the cathode must have a crystal structure with suitable crystallographic sites for Zn^{2+} accommodation, low-energy paths for ion diffusion, and high electronic conductivity for charge transfer [6]. To meet these requirements, layered and tunnel structured compounds with redox components are often chosen. In this case, the cathode must also have sufficient porosity to allow the penetration of the electrolyte solution, thereby increasing the number of active sites for the maximum charge transfer rate [7]. The materials that meet the presented requirements include analogs of Prussian blue, manganese and cobalt oxides, vanadium oxides, as well as organic compounds [8–10]. Among these materials, manganese oxides are of the greatest interest from the point of view of their further commercialization, since they have a high specific capacity and a wide working potential window, while they can be synthesized from relatively inexpensive precursors [11, 12]. However, these cathode materials have low electronic conductivity, which does not allow them to approach the theoretical values of the specific capacitance.

The solution to this problem may consist of obtaining 2D nanocrystals with a graphene-like morphology of the so-called "nanosheets", which is due to a set of their unique physical and chemical properties. The flat 2D structure of such materials provides a sufficient number of active adsorption centers. Another key characteristic of 2D materials is their ultra-small thickness, on the order of a few nanometers, so charge carriers can travel extremely short distances from the volume to the surface, while significantly improving electronic conductivity [13–15].

New possibilities of manganese oxides nanocrystals synthesis rose after the development of Layer-by-Layer (LbL) synthesis techniques that make it possible to deposit MnO$_2$ layers on the surface of samples with an irregular shape, providing an exact thickness of the layer [16]. The purpose of the present study was to explore the feasibility of synthesis of the MnO$_2$ nanolayers by the Successive Ionic Layer Deposition (SILD) method [17], also called the Successive Ionic Layer Adsorption and Reaction (SILAR) [18]. The method is based on multiple and successive treatments of a substrate by solutions of reagents which enter into reaction at its surface and form a layer of poorly soluble substance. The distinctive features of this method are its capability of deposition of the layers of controlled thickness on the surface of parts of any shape, which are exactly the requirements to the methods of synthesis of the layers on the surface of electrodes for the zinc-ion battery.

In the present paper, we report a new simple oxidation-reduction route for the synthesis of Zn-doped MnO$_2$ nanolayers via the SILD method. The obtained nanolayers consist of MnO$_2$ nanocrystals, including zinc atoms, with nanosheets-like morphology. We also describe their properties as electroactive cathode materials for an aqueous zinc-ion battery.

2. Experimental

As a substrate for the synthesis of Zn-doped MnO$_2$ nanolayers $0.3 \times 5 \times 25$ mm polycrystalline Ni foam (NF) (110 ppi) plates were used, on which electrochemical experiments were performed, and also $0.35 \times 10 \times 25$ mm single-crystal Si plates with $\langle 100 \rangle$ orientation, were used for physical characterization. Extra pure water (Milli-Q) was used in all experiments. Si substrates were cleaned in an ultrasonic bath filled with acetone for 10 min. Then plates of Si were sequentially treated for 10 min in concentrated HF, water, 70% HNO$_3$, water, 0.1 M KOH and then flushed out by water. Ni plates were treated according to the technique described in [19] for 15 min in 6 M HCl solution, then several times rinsed by water and dried on air at 120°C for 30 min.

A solution of mixed salts manganese and zinc was prepared by dissolving dry analytical grade salts MnSO$_4$ and ZnSO$_4$ ($C = 0.01$ M) in deionized water. An aqueous solution of NaClO ($C = 0.01$ M) was used as an oxidizer. The pH of this solution was 10.5 and adjusted by the addition of 1M NaOH solution. For the synthesis of Zn-doped MnO$_2$ nanolayers, substrate plates were sequentially immersed for 30 seconds into a solution of mixed manganese and zinc salt, washed in water, and then it was immersed for 30 seconds into the NaClO solutionand again washed in water. The sequence corresponds to one SILD cycle, which is repeated 30 times to obtain desired film thickness. Then samples were calcined on air at 150°C for 10 min at a heating rate of 5°C/min.

The morphology and composition of synthesized films were investigated by scanning electron microscope (SEM) at accelerating voltage 1–10 kV on Zeiss Merlin microscope and X-ray photoelectron spectroscopy (XPS) was obtained used ESCALAB 250Xi electron spectrometer, with Al Kα radiation (14866 eV). XRD patterns were obtained using a Rigaku Miniflex II X-ray diffractometer with CuKα radiation ($\lambda = 0.154056$ nm). FT-IR transmission spectra of synthesized films on silicon surface were registered by FCM-2201 spectrophotometer using a different technique with respect to spectra of bare silicon plate.

The electrochemical measurements of NF electrodes with the synthesized nanolayers were carried out in a two-electrode electrochemical cell using Elins P-45X potentiostat. The cathode was prepared by deposition Zn-doped MnO$_2$ nanolayers on NF surface as a result of 30 treatment cycles by the SILD method. Zinc foil serves as an anode. Electrochemical characterization of the films was made by cyclic voltammetry (CV) and galvanostatic charge-discharge (CD) techniques.

The specific capacitance C (mAh/g) as an electrode for alkaline battery at different current densities can be calculated via eq (1):

$$C = \int \frac{I \mathrm{d}t}{m} \tag{1}$$

where I (mA) is a galvanostatic current, $\mathrm{d}t(h)$ is the discharge time of a cycle and $m(g)$ is the mass of the active material in the film electrode [20]. The electroactive mass of Zn-doped MnO$_2$ for the cathode was measured using an OHAUS Pioneer ^{TM} PA54C microbalance.

3. Results and discussion

Morphological characteristics of the sample are shown in the SEM images in Fig. 1. The layer was synthesized on the nickel foam via the SILD method by 30 cycles of treatment. It is clear from the image that the layers formed of nanocrystals with nanosheets-like morphology with a thickness of 3–8 nm. Synthesized nanolayer has a uniform dark brown color.

On the X-ray diffraction pattern of the synthesized sample (Fig. 2) the crystallographic planes (001), (002), and (-111) is corresponding to the birnessite-like crystal phase of MnO$_2$ (JCPDS 42-1317) [21].

In the FTIR spectrum (Fig. 3), one can observe absorption bands with maximums at 3400 and 1620 cm^{-1} referring to valence oscillations of O–H groups in the molecules of adsorbed water [22]. The band with a maximum of about 440 cm^{-1} results from valence oscillations of manganese-oxygen bonds in MnO$_2$ [23].

The X-ray photoelectron spectra of the synthesized sample are shown in Fig. 4. Following the results of Ref. [24] the peaks at 642.1 eV (Mn $2p_{3/2}$) and 653.8 eV (Mn $2p_{1/2}$) in these spectra for the Mn $2p$ electrons with an energy separation ΔE of 11.7 eV (Fig. 4a) and energy separation of Mn $3s$ ($\Delta E = 5.1$ eV Fig. 4b) may be assigned to manganese atoms in the 4+ oxidation state [25]. The peak at 529.5 eV (Fig. 4c) corresponding to atoms of oxygen in the manganese oxide crystalline lattice, respectively [26]. The XPS spectrum also indicates the presence of Zn and Mn elements with an atomic ratio of 0.3/1.0.
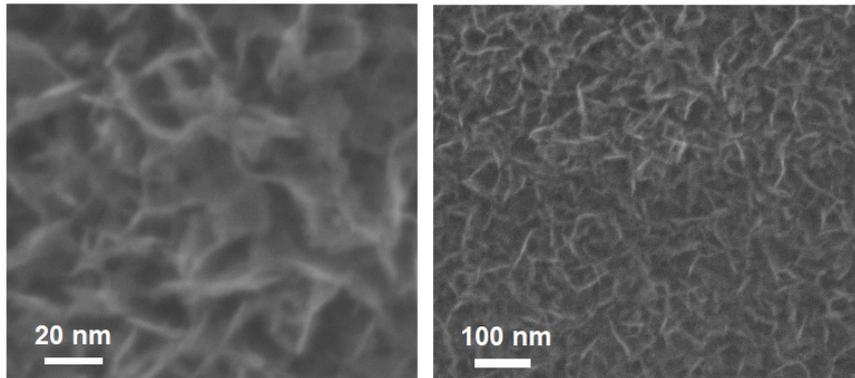
FIG. 1. SEM images of manganese contained nanolayers
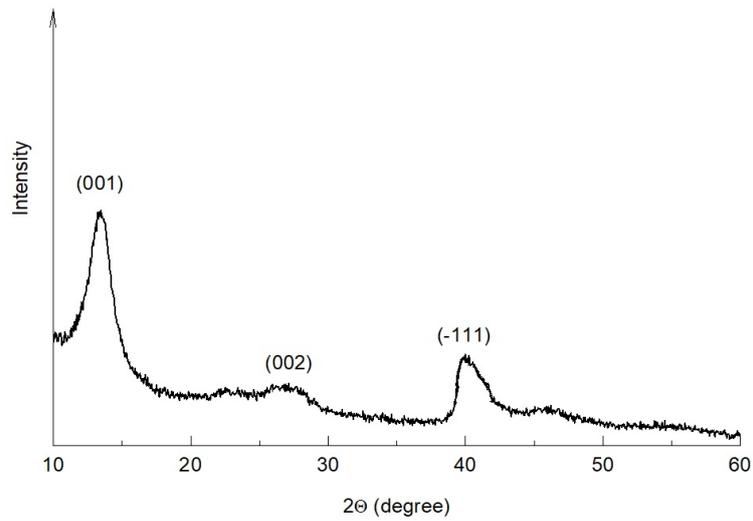
FIG. 2. XRD patterns of manganese contained nanolayers
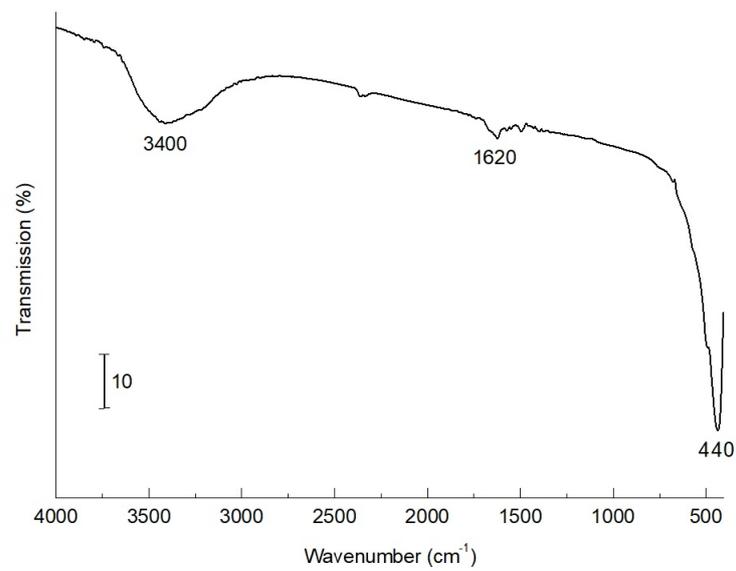
FIG. 3. FTIR transmission spectra of manganese contained nanolayers on a silicon surface
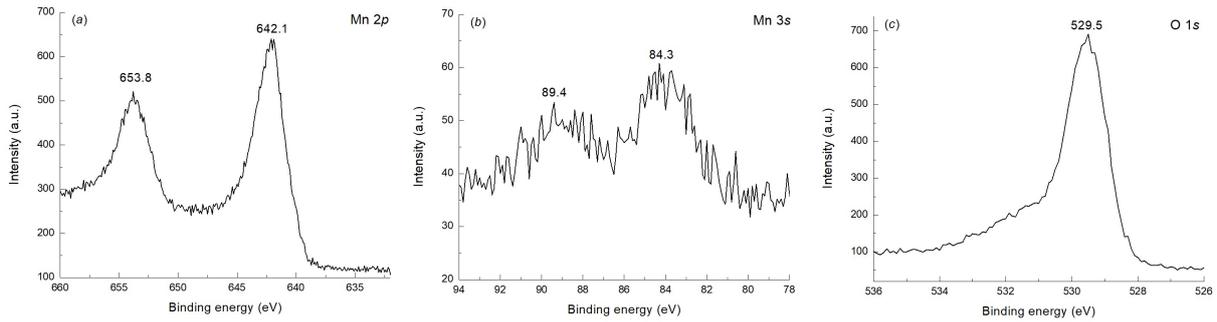
FIG. 4. XPS spectra Mn 2p (a), Mn 3s (b) and O 1s (c) of manganese contained nanolayers on a silicon surface

Comparison of research results, conducted via XRD, XPS and FTIR methods, allows us to conclude: obtained nanolayers consist of manganese oxide, doped zinc atoms, which are likely to be included in the crystal structure of birnessite MnO$_2$. Based on these results, we propose a formula synthesized layer as Zn$_{0.3}$MnO$_2$.

For explaining the obtained results, a description of chemical reactions, occurring on the surface can be suggested. At the first step, after dipping in the solution of mixed salts, MnSO$_4$ and ZnSO$_4$ on the surface occur adsorption of cations Mn$_{aq}^{2+}$ and Zn$_{aq}^{2+}$. Then, after treatment in the solution of NaClO, these cations form on the surface of the nucleus of the MnO$_2$ nanocrystals, which are then, after treatment in the solution of MnSO$_4$, on the second SILD cycle form layered birnessite-like MnO$_2$ nanocrystal with Zn^{2+} ions in the interlayer space. After several repetitions of SILD cycles, the number of such nanocrystals and their length increases from the so-called nanosheets morphology.

We assume that such structure can possess interesting and practical electrochemical performance as cathode materials of aqueous zinc-ion battery. The cyclic voltammograms of the NF electrode with Zn-doped MnO$_2$ nanolayer were recorded in a potential window from 500 to 2000 mV vs. Zn/Zn^{2+} electrode in 2M ZnSO$_4$ electrolyte at scanning rates of 5, 10 and 15 mV/s (Fig. 5). At a scan rate of 5 mV/s, two electrochemical processes take place in the layer, including the intercalation of zinc ions at 1780 mV and their de-intercalation at 1230 mV. The proportionality of currents to scan rate provides information that the film is thick enough, and the charge transfer rate is limited by diffusion of charge carriers in the film.
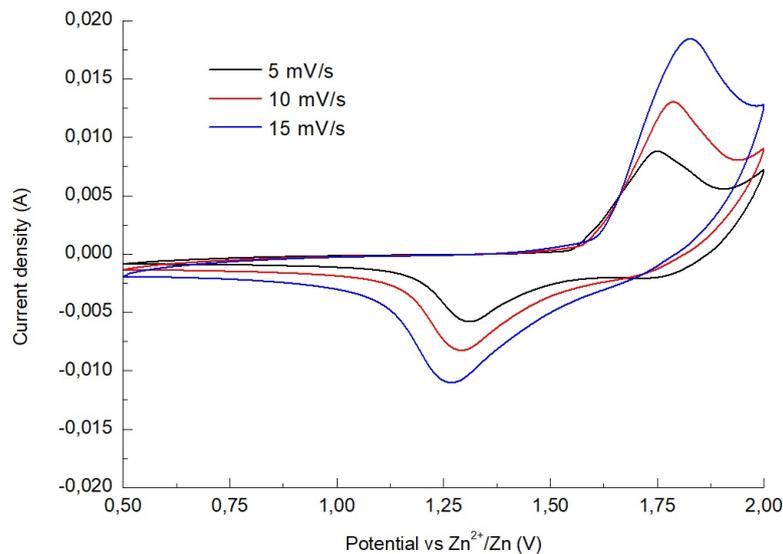
FIG. 5. CVA curves for NF electrode with Zn-doped MnO$_2$ nanolayers at a scan rate of 5, 10 and 15 mV/s

The specific capacitance of the Zn-doped MnO$_2$ NF electrode is calculated from charge-discharge curves (Fig. 6) by eq (1) to be 216 mAh/g at the current densities of 1 A/g. The high value of specific capacity can be explaining by

the good conductivity of MnO_2 nanosheets and also the significant influence of zinc atoms on the crystal structure of the sample.
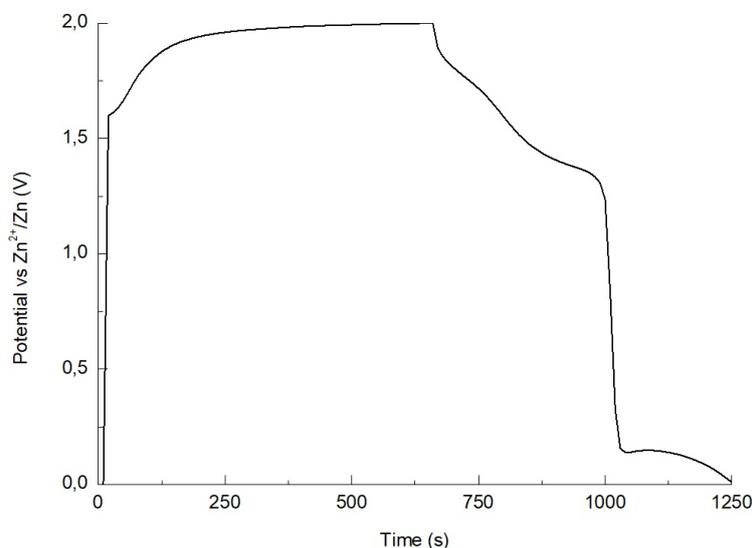
FIG. 6. Galvanostatic charge-discharge curve (at the current densities of 1 A/g) of the electrode with Zn-doped MnO_2 nanolayers

Cyclic stability is also an important property for electroactive materials. The capacity retention of NF electrode with Zn-doped MnO_2 nanolayer after 1000 charge-discharge cycles at a current density of 1 A/g maintained 95% of its initial capacity, which shows good cycling stability of this material. High cycling stability can be explained feature morphology of ultrathin nanocrystals of MnO_2 which provide fast diffusion of zinc ions and while not being destroyed.

The high value of specific capacitance for the electrodes synthesized by the SILD method can be explained, in our opinion, by the relatively smaller size of oxide nanocrystals formed during the layer deposition, which enlarges the effective surface area of the electrode,and consequently, results in the higher specific capacitance. Additionally, the smaller size of nanocrystals brings about good intercalation/de-intercalation of zinc ions on the electrode surface and hence affects positively the electrochemical stability. We believe that these electrochemical capacity characteristics of Zn-doped MnO_2 nanocrystals, synthesized via the SILD method, can be improved through a new scheme of their synthesis, including nanocomposite with carbon materials (CNT, graphene) formation that has been obtained after a new sequence of reagent treatment. However, these experiments fall beyond the scope of the present paper.

4. Conclusion

In summary, the possibility was shown forobtaining Zn-doped MnO_2 nanolayers via the SILD method used mixed manganese and zinc salts aqueous solution and NaClO as an oxidant. The results show the synthesized nanolayers were formed nanocrystals of the thickness of about 3–8 nm with the nanosheets morphology and the monoclinic birnessite-like crystal structure of MnO_2. The electrochemical study of Zn-doped MnO_2 nanolayers-modified nickel foam electrodes, prepared by 30 SILD cycles, demonstrates that the specific capacitance is 216 mAh/g at a current density of 1 A/g. Repeated cycling for 1000 charge-discharge cycles demonstrates a relatively small 5% capacitance fade. Thus this material can be potentially applied as an effective electroactive material for an aqueous zinc-ion battery.

Acknowledgements

References

[1] Kaiyue Zhu, Tao Wu, Shichen Sun, Yeting Wen, Kevin Huang. Electrode Materials for Practical Rechargeable Aqueous Zn Ion Batteries. *Challenges and Opportunities, ChemElectroChem*, 2020, 7, P. 2714–2734.

[2] Jianping Yan, Edison Huixiang Ang, Yang Yang, Yufei Zhang, Minghui Ye, Wencheng Du, Cheng Chao Li. High Voltage Zinc Ion Batteries. *Design Strategies and Challenges, Advanced Functional Materials*, 2021, **335**, P. 2010213.

[3] Yanxia Yu, Jinhao Xie, Haozhe Zhang, Ruofei Qin, Xiaoqing Liu, Xihong Lu. High Voltage Rechargeable Aqueous Zinc Based Batteries. *Latest Progress and Future Perspectives, Small Science*, 2021, **355**, P. 2000066.

[4] Niklas Borchers, Simon Clark, Birger Horstmann, Kaushik Jayasayee, Mari Juel, Philippe Stevens.Innovative zinc-based batteries. *Journal of Power Sources*, 2021, **484**, P. 229309.

[5] Nengyan Ma, Peijun Wu, Yixue Wu, Donghao Jiang, Gangtie Lei. Progress and perspective of aqueous zinc-ion battery. *Functional Materials Letters*, 2019, **12**(5), P. 1930003.

[6] Dinesh Selvakumarana, Anqiang Pana, Shuquan Lianga, Guozhong Cao. A review on recent developments and challenges of cathode materials for rechargeable aqueous Zn-ion batteries. *J. Mater. Chem. A*, 2019, **7**, P. 18209–18236.

[7] Zixuan Fan, Wei He, Meng Ni, Peigeng Zhang, Wubian Tian, Wei Zhang, Long Pan, ZhengMing Sun. Recent Developments of Preintercalated Cathodes for Rechargeable Aqueous Zn-Ion Batteries. *Energy Technol*, 2021, **9**, P. 2000829.

[8] Wen Shi, Wee Siang Vincent Lee, Junmin Xue. Recent Development of Mn-based Oxides as Zinc-Ion Battery Cathode. *ChemSusChem*, 2021, **14**, P. 1–26.

[9] Muhammad Rashad, Muhammad Asif, Yuxin Wang, Zhen He, Iftikhar Ahmed. Recent advances in electrolytes and cathode materials for magnesium and hybrid-ion batteries. *Energy Storage Materials*, 2020, **25**, P. 342–375.

[10] Na Liu, Bin Li, Zhangxing He, Lei Dai, Haiyan Wang, Ling Wang. Recent advances and perspectives on vanadium- and manganese-based cathode materials for aqueous zinc ion batteries. *Journal of Energy Chemistry*, 2021, **59**, P. 134–159.

[11] Tong Xue, Hong Jin Fan, From aqueous Zn-ion battery to Zn-MnO$_2$ flow battery: A brief story. *Journal of Energy Chemistry*, 2021, **54**, P. 194–201.

[12] Boya Tang, Lutong Shan, Shuquan Liang, Jiang Zhou. Issues and opportunities facing aqueous zinc-ion batteries. *Energy Environ. Sci.*, 2019, **12**, P. 3288.

[13] Yingchang Yang, Xuejing Qiu, Wei Shi at all. Controllable fabrication of two-dimensional layered transition metal oxides through electro-chemical exfoliation of non-van der Waals metals for rechargeable zinc-ion batteries. *Chemical Engineering Journal*, 2021, **15**, P. 127247.

[14] Huicong Xia, Qun Xu, Jianan Zhang. Recent Progress on Two-Dimensional Nanoflake Ensembles for Energy Storage Applications. *Nanomicro Lett.*, 2018, **10**.

[15] Wang Xiao, Li Yaguang, Wang Sen, Zhou Feng, Das Pratteek, Sun Chenglin, Zheng Shuanghao, Wu Zhong Shuai. 2D Amorphous V$_2$O$_5$/Graphene Heterostructures for High Safety Aqueous Zn Ion Batteries with Unprecedented Capacity and Ultrahigh Rate Capability. *Advanced energy materials*, 2020, **10**.

[16] Shamsayei M., Yamini Y., Asiabi H. Layer-by-layer assembly of layered double hydroxide/histidine/δ-MnO$_2$ nanosheets: Synthesis, charac-terization, and applications. *Applied Clay Science*, 2020, **188**, P. 105540.

[17] Kodintsev I.A., Martinson K.D., Lobinsky A.A., Popkov V.I. SILD synthesis of the efficient and stable electrocatalyst based on CoO-NiO solid solution toward hydrogen production. *Nanosystems: Physics, Chemistry, Mathematics*, 2019, **10**(6), P. 681–685.

[18] Mangesh A. Desai, Aditi Kulkarni, Girish Gund, Shrikrishna. D. Sartale, SILAR-grown K+ and Na+ions pre-inserted MnO$_2$ nanostructures for supercapacitor applications: A comparative study. *Energy Fuels*, 2021, **35**, P. 4577–4586.

[19] Tolstoy V.P., Lobinsky A.A., Levin O.V., Kuklo L.I. Direct synthesis of Ni$_2$Al(OH)$_{7-x}$(NO$_3$)$_x$·nH$_2$O layered double hydroxide nanolayers by SILD and their capacitive performance. *Materials Letters*, 2015, **139**, P. 4–6.

[20] Tolstoy V.P., Lobinsky A.A. Synthesis of 2D Zn-Co LDH nanosheets by a successive ionic layer deposition method as a material for electrodes of high-performance alkaline battery-supercapacitor hybrid devices. *RSC Advances*, 2018, **8**, P. 29607–29612.

[21] Hongjun Yue, Xingkang Huang, Yong Yang. Preparation and electrochemical performance of manganese oxide/carbon nanotubes composite as a cathode for rechargeable lithium battery with high power density. *Mater. Lett.*, 2008, **62**, P. 3388–3390.

[22] Kodintsev I.A., Martinson K.D., Lobinsky A.A., Popkov V.I. Successive ionic layer deposition of Co-doped Cu(OH)$_2$ nanorods as electrode material for electrocatalytic reforming of ethanol. *Nanosystems: Physics, Chemistry, Mathematics*, 2019, **10**(5), P. 573–578.

[23] Yu Xin Zhang, Xiao Long Guo, Ming Huang, Xiao-Dong Hao, Yuan Yuan, Chao Hua. Engineering birnessite-type MnO$_2$ nanosheets on fiberglass for pH-dependent degradation of methylene blue. *J. Phys. and Chem. of Sol.*, 2015, **83**, P. 40–46.

[24] Shumin Sun, Shen Wang, Tongchi Xia, Xiaofeng Li, Qingxian Jin, Qiong Wu. Hydrothermal synthesis of a MnOOH/three-dimensional reduced graphene oxide composite and its electrochemical properties for supercapacitors. *J. Mater. Chem. A.*, 2015, **3**, P. 20944–20951.

[25] Biesinger M.C., Payne B.P., Grosvenor A.P., Lau L.W.M., Gerson A.R., Smart R.St.C. Resolving surface chemical states in XPS analysis of first-row transition metals, oxides and hydroxides: Cr, Mn, Fe, Co and Ni. *Appl. Surf. Sci.*, 2011, **257**, P. 2717–2730.

[26] Lobinsky A.A., Tolstoy V.P. Synthesis of γ-MnOOH nanorods by successive ionic layer deposition method and their capacitive performance. *Journal of Energy Chemistry*, 2017, **26**, P. 336–339.